

UC Davis

UC Davis Previously Published Works

Title

Calmodulin promotes a Ca²⁺-dependent conformational change in the C-terminal regulatory domain of CaV1.2

Permalink

<https://escholarship.org/uc/item/0mz302bd>

Journal

FEBS Letters, 596(22)

ISSN

0014-5793

Authors

Yadav, Deepak Kumar

Anderson, David E

Hell, Johannes W

et al.

Publication Date

2022-11-01

DOI

10.1002/1873-3468.14529



Copyright Information

This work is made available under the terms of a Creative Commons Attribution License, available at <https://creativecommons.org/licenses/by/4.0/>

Peer reviewed

RESEARCH LETTER

Calmodulin promotes a Ca²⁺-dependent conformational change in the C-terminal regulatory domain of Ca_v1.2

 Deepak Kumar Yadav¹ , David E. Anderson¹, Johannes W. Hell² and James B. Ames¹ 
¹ Department of Chemistry, University of California, Davis, CA, USA

² Department of Pharmacology, University of California, Davis, CA, USA

Correspondence

J. B. Ames and D. K. Yadav, Department of Chemistry, University of California, One Shields Avenue, Davis, CA 95616, USA
 Tel: +1 530 752 6358
 E-mails: jbam@ucdavis.edu (JBA); dkyadav@ucdavis.edu (DKY)

(Received 9 September 2022, revised 7 October 2022, accepted 10 October 2022)

doi:10.1002/1873-3468.14529

Edited by Maurice Montal

Calmodulin (CaM) binds to the membrane-proximal cytosolic C-terminal domain of Ca_v1.2 (residues 1520–1669, CT(1520–1669)) and causes Ca²⁺-induced conformational changes that promote Ca²⁺-dependent channel inactivation (CDI). We report biophysical studies that probe the structural interaction between CT(1520–1669) and CaM. The recombinantly expressed CT(1520–1669) is insoluble, but can be solubilized in the presence of Ca²⁺-saturated CaM (Ca₄/CaM), but not in the presence of Ca²⁺-free CaM (apoCaM). We show that half-calcified CaM (Ca₂/CaM₁₂) forms a complex with CT(1520–1669) that is less soluble than CT(1520–1669) bound to Ca₄/CaM. The NMR spectrum of CT(1520–1669) reveals spectral differences caused by the binding of Ca₂/CaM₁₂ versus Ca₄/CaM, suggesting that the binding of Ca²⁺ to the CaM N-lobe may induce a conformational change in CT(1520–1669).

Keywords: calmodulin; Ca_v1.2; Ca_v1.4; IQ-switch; L-type Ca²⁺ channel; NMR

Long-lasting (L-type) voltage-gated Ca²⁺ channel (Ca_v1.2) regulates neuronal excitability in the brain and heart [1]. The activation of Ca_v1.2 channels elicits several Ca²⁺-dependent biological processes, including gene transcription [2], neurite outgrowth in neuron cells [3], release of neurotransmitter [4], and Ca²⁺-dependent enzyme activation [5]. The Ca²⁺-dependent Ca_v1.2 channel activity is regulated by calmodulin (CaM) [6]. CaM binding to the IQ-motif of Ca_v1.2 promotes Ca²⁺-dependent channel inactivation (CDI) [7,8 and others] and augments channel open probability at basal Ca²⁺ levels [9]. Defects in the Ca²⁺-dependent Ca_v1.2 channel regulation are associated with several disorders such as arrhythmia, autism spectrum disorders including Timothy's syndrome [10,11], and epilepsy [12].

Ca_v1.2 is a multimeric complex consisting of a transmembrane α1-subunit, cytosolic β-subunit, and extracellular α2-subunit. The α1-subunit contains four transmembrane domains (I–IV, Fig. 1A) and a long cytosolic C-terminal tail called the CT-domain (Fig. 1A). The cytosolic CT-domain consists of two EF-hands, pre-IQ, IQ-motif, and proximal C-terminal regulatory domain (PCRD) (Fig. 1A). The Cryo-EM structure of the closely related L-type Ca²⁺ channel Ca_v1.1 [13,14] revealed a linker between domains III and IV that contacts the two EF hands, which may form a plug at the channel entrance to cause channel inactivation [6]. The interaction between the III–IV linker and CT-domain might be controlled by the binding of CaM. Unfortunately, the CaM binding to the IQ-motif and all residues downstream of the pre-IQ

Abbreviations

BME, β-mercaptoethanol; CaCl₂, calcium chloride; CaM, calmodulin; CDI, Ca²⁺-dependent channel inactivation; EGTA, ethylene glycol-bis(β-aminoethyl ether)-N,N,N',N'-tetraacetic acid; HSQC, heteronuclear single quantum coherence; IPTG, isopropyl β-D-1-thiogalactopyranoside; KCl, potassium chloride; NMR, nuclear magnetic resonance; SEC, size exclusion chromatography; TCEP, tris(2-carboxyethyl)phosphine.

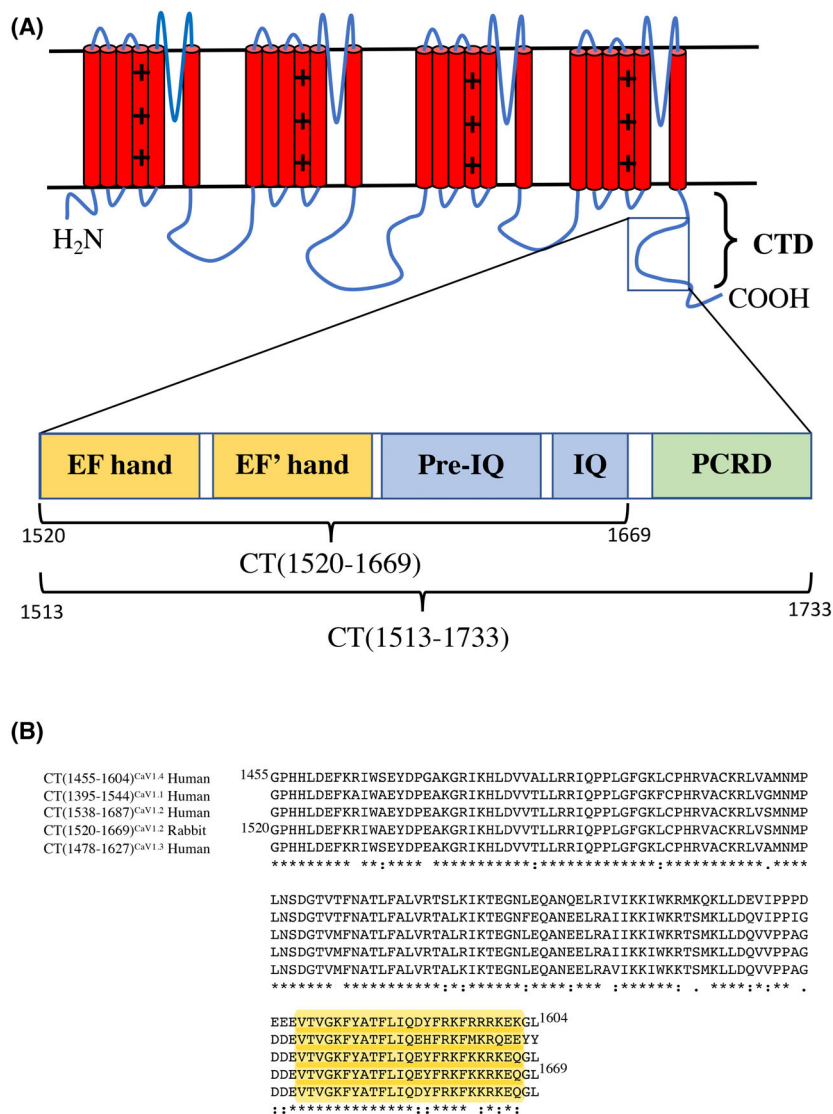


Fig. 1. Schematic representation of the C-terminal domain of L-type Ca²⁺ channels and amino acid sequence alignment of Ca_vs. (A) Transmembrane α -helices of the four subunits of Ca_vs (red), cytoplasmic loops (blue), and C-terminal regulatory domain (CTD). CTD region is comprised of EF hands (yellow), pre-IQ and IQ (blue) and PCRD (green). Amino acid sequence numbers of CT domains are labelled according to rabbit Ca_v1.2. (B) CT(1520–1669) amino acid sequence (150 amino acid region) of different Ca_vs [CT(1395–1544)^{CaV1.1} Human (spI Q13698ICAC1S); CT(1538–1687)^{CaV1.2} Human (spIQ13936ICAC1C); CT(1478–1627)^{CaV1.3} Human (spIQ01668ICAC1D); CT(1455–1604)^{CaV1.4} Human (spIO60840ICAC1F); CT(1520–1669)^{CaV1.2} Rabbit (spIP15381ICAC1C)] were aligned using CLUSTAL OMEGA (<https://www.ebi.ac.uk/Tools/msa/clustalo/>) with IQ-region highlighted in yellow.

are dynamically disordered or otherwise undetected in the cryo-EM structure of Ca_v1.1 [13,14]. A crystal structure is known for CaM bound to a peptide fragment of the IQ-motif [15], but the structure of CaM bound to the full-length Ca_v1.2 is currently not known. An atomic-level structure of Ca_v1.2 bound to CaM is critical for understanding the mechanism of CDI.

Ideally, we would like to solve the atomic-level structure of CaM bound to the full-length Ca_v1.2, but the

CaM binding site remains structurally disordered in the cryo-EM structure even in the presence of CaM [13,14]. Instead, we present a structural analysis of a fragment of the Ca_v1.2 CT-domain that includes two EF-hands, the pre-IQ and IQ-motif (residues 1520–1669, called CT (1520–1669)). The amino acid sequence alignment of CT (1520–1669) with the different L-type Ca²⁺ channels shows a highly conserved IQ-motif region (90% identity in Fig. 1B, highlighted in yellow), whereas the EF hand and pre-IQ regions are slightly less conserved (80%

identity) between Ca_v1.2 and Ca_v1.4 (Fig. 1B). The recombinant CT(1520–1669) alone is not soluble enough for structural studies, but the CT(1520–1669) solubilized by 8 M urea can be refolded in a soluble form in the presence of Ca²⁺-saturated CaM (Ca₄/CaM), but not in the presence of apoCaM [16]. In this study, we show that half-calcified CaM (Ca₂/CaM₁₂) forms a complex with CT(1520–1669) that is less soluble than CT(1520–1669) bound to Ca₄/CaM. The binding of CaM to CT(1520–1669) forms at least a tetrameric complex in which four CaM are bound to four CT(1520–1669). NMR spectra of ¹⁵N-labelled CT(1520–1669) bound to unlabelled CaM reveal spectral differences caused by Ca₂/CaM₁₂ versus Ca₄/CaM binding, suggesting a CaM-induced conformational change in CT(1520–1669). These results support the recently proposed IQ-switch model for CDI [6].

Materials and methods

Plasmids used for protein expression

The CaM, CaM₁₂ (Ca²⁺ binding sites in the N-lobe are mutated as D21A/D23A/D25A/E32Q/D57A/D59A/N61A/E68Q so that only the C-lobe can bind Ca²⁺) and CaM_C (only C-lobe of CaM) expression plasmids were subcloned into pET11b expression vector (Novagen, Millipore Sigma, Burlington, MA, USA) as described in Bartels et al., [17]. The CT(1513–1733) expression plasmid was subcloned into pET24 expression vector (Novagen) from GST-CT-domain in pGEX vector (gift of Johannes W. Hell lab, UC Davis). CT(1520–1669) constructs were subcloned into the expression vector pMA507, a gift from Mark Arbing, David Eisenberg lab UCLA [18] using sequence and ligation independent method as described previously [19,20]. The C-terminal region of Ca_v1.4 (two channel EF-hands, pre-IQ and IQ-motif: residues 1455–1604 called CT(1455–1604)^{CaV1.4}) was also subcloned into pMA507 expression vector. The recombinantly expressed proteins CT(1520–1669) and CT(1455–1604)^{CaV1.4} each contain a TEV cleavable N-terminal 6His-tag, whereas CT(1513–1733) contains an uncleavable C-terminal 6His-tag.

Protein expression and purification

A single *Escherichia coli* colony from an overnight grown streak plate (either BL21 DE3 or Rosetta 2) was inoculated into 15 mL LB-broth containing antibiotics and grown at 37 °C overnight. This pre-culture was added to 1 L of LB-broth containing antibiotics and the cells grown at 37 °C until A₆₀₀ = 0.5–0.8, then 1 mM IPTG was added to induce protein expression. Cells were harvested by centrifugation, resuspended in lysis buffer, and stored at –80 °C. After thawing, the cell pellet was mixed with one tablet of protease inhibitor cocktail (Roche, Basel, Switzerland), and the

cell suspension was disrupted by sonication. Inclusion bodies were sedimented by centrifugation and the pellet was rinsed with wash buffer containing 20 mM Tris pH 7.5, 1 M urea, 0.15 M KCl, 2 mM TCEP. After spinning down insoluble material by centrifugation, the pellet was re-suspended with solubilizing buffer containing 20 mM Tris pH 7.5, 8 M urea, 0.15 M KCl, 2 mM TCEP, homogenized, and incubated for 30 min at room temperature. Any remaining insoluble protein was spun down and the supernatant was applied onto a Ni-NTA column equilibrated with solubilizing buffer. The Ni-NTA column was washed with 3–5 column volumes of solubilizing buffer, then further washed with the same buffer containing 25 mM imidazole to remove any impurities. Protein was eluted with buffer containing 20 mM Tris pH 7.5, 8 M urea, 0.75 M Imidazole, 0.15 M KCl, 2 mM TCEP. CaM was expressed and purified as described previously in Turner et al. (2020) [21] and the same procedure was followed for CaM₁₂ and CaM_C.

Refolding of protein complexes and gel electrophoresis

The CT(1520–1669) (or CT(1455–1604)^{CaV1.4} or CT(1513–1733)) was mixed with 1 or 3 equivalents of purified CaM, CaM₁₂ or CaM_C separately, each in the presence of 2 mM CaCl₂. For the control reaction mixture, CT(1520–1669) (or CT(1455–1604)^{CaV1.4} or CT(1513–1733)) were mixed with 1 or 3 equivalents purified apoCaM in the presence of 2 mM EGTA. For protein refolding, the reaction mixture was dialysed twice against 2 L dialysis buffer containing 20 mM Tris pH 7.5, 0.15 M KCl, 2.0 mM CaCl₂, 2 mM BME for calcified CaMs, and 20 mM Tris pH 7.5, 0.15 M KCl, 2.0 mM EGTA, 2 mM BME for apoCaM. Any precipitated complex in the dialysate was sedimented by centrifugation and washed again with dialysis buffer. After collecting the soluble solution and insoluble pellet, the protein complex was analysed by SDS/PAGE. SDS/PAGE was run using commercial gels (Invitrogen, Thermo Fisher Scientific, Waltham, MA, USA) and each sample was mixed 1 : 1 with SDS/PAGE treatment buffer. The gel was stained with Coomassie brilliant blue R-250. Complexes were further purified by size exclusion chromatography before NMR measurements.

NMR spectroscopy and size exclusion chromatography

The 2D ¹H-¹⁵N HSQC NMR spectrum was measured using a Bruker Avance III 600 or 800 MHz (Bruker, San Jose, CA, USA) spectrometer at 37 °C. NMR samples of complexes were prepared by purifying through size exclusion (S75) column chromatography and exchanged with NMR buffer: 20 mM Tris-d11 pH 7.5, 0.1 M KCl, 1.0 mM CaCl₂, 2 mM DTT-d10, 10% D₂O. For the NMR sample, ¹⁵N-labelled CT(1520–1669) (or CT(1455–1604)^{CaV1.4} or CT(1513–1733)) was refolded in the presence of more than 3-

fold excess unlabelled CaM_s as described above. To remove excess CaMs, we ran size exclusion (S75) column chromatography at 4 °C with SEC buffer: 20 mM Tris pH 7.5, 0.1 M KCl, 1.0 mM CaCl₂, 2 mM BME. Fractions with both protein bands on SDS/PAGE were pooled and concentrated down to 500 μL for NMR measurements. ¹⁵N-labelled CT(1520–1669), CT(1455–1604)^{CaV1.4}, and CT(1513–1733) samples were overexpressed in M9 minimal media, containing 1 g·L⁻¹ ¹⁵NH₄Cl (Cambridge Isotopes Laboratories, Tewksbury, MA, USA) as described in the above section for the expression in LB-broth. NMR data were processed and visualized by using software TOPSPIN 3.6.1 (Bruker), NMRFX [22], and NMRVIEW [23].

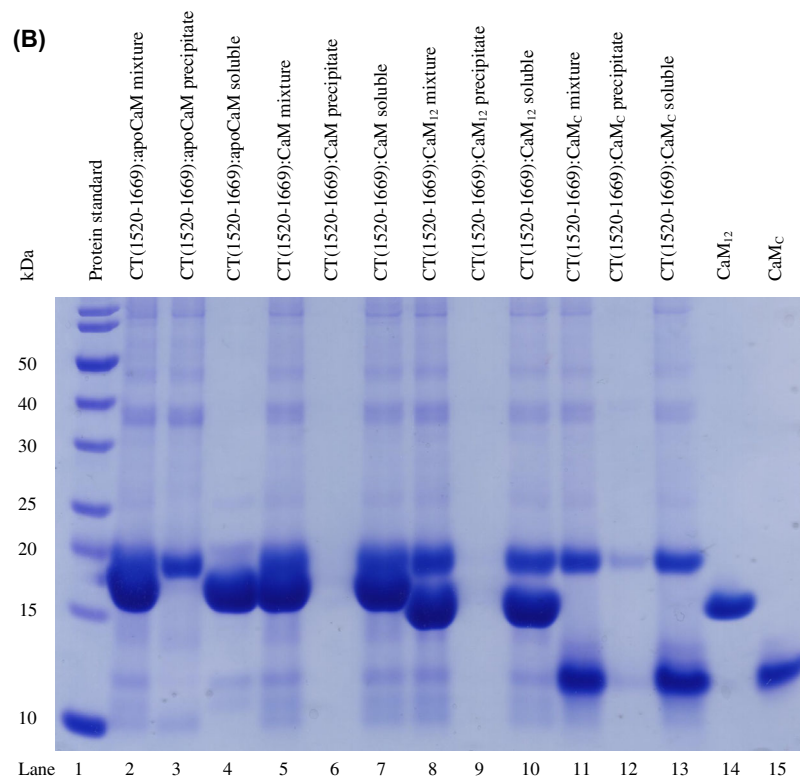
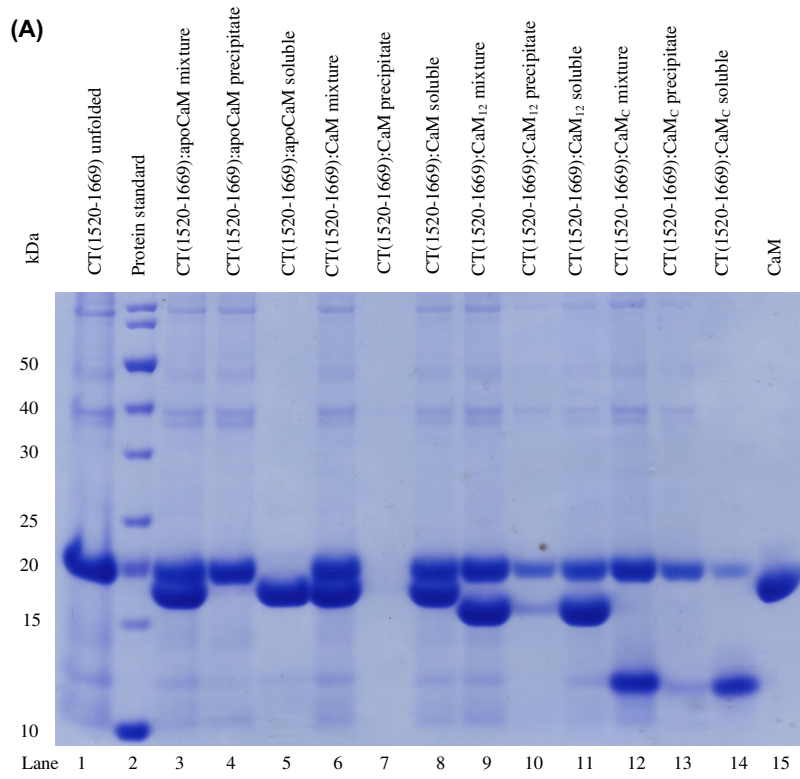
Results

Refolding of CT(1520–1669) (and CT(1513–1733)) in the presence of Ca₄/CaM, Ca₂/CaM₁₂, and Ca₂/CaM_C

The recombinantly expressed C-terminal domain of Ca_v1.2 that includes two channel EF-hand motifs, pre-IQ and IQ-motif (residues 1520–1669, called CT(1520–1669)), or a similar construct that contained the proximal C-terminal regulatory domain (residues 1513–1733, called CT(1513–1733)) were not soluble as described by Xiong et al. [16]. To form a soluble complex of CT(1520–1669) bound to CaM, the urea-solubilized CT(1520–1669) (or CT(1513–1733)) was refolded by dialysing away the urea in the presence of CaM. The CT(1520–1669) domain refolding in the presence of apoCaM (2 mM EGTA) caused the CT(1520–1669) protein to precipitate without binding to CaM (Fig. 2A, lane 4), indicating that apoCaM does not bind strongly

enough to solubilize the tertiary complex. Increasing the apoCaM concentration by 3-fold still was not able to solubilize CT(1520–1669) (Fig. 2B, lane 4). By contrast, if Ca²⁺-saturated CaM (Ca₄/CaM) is added to the urea-solubilized CT(1520–1669) domain, then the refolding of CT(1520–1669) (during dialysis) forms a soluble tertiary complex CT(1520–1669):Ca₄/CaM (Fig. 2A, lane 8). Half-calcified CaM (Ca₂/CaM₁₂) and Ca²⁺-bound CaM C-lobe (Ca₂/CaM_C) solubilized about 50% of the tertiary complexes (CT(1520–1669):Ca₂/CaM₁₂ or CT(1520–1669):Ca₂/CaM_C) as shown in Fig. 2A lane 11 and lane 14, respectively. The remaining 50% of the tertiary complexes (CT(1520–1669):Ca₂/CaM₁₂ and CT(1520–1669):Ca₂/CaM_C) was insoluble as shown in Fig. 2A lane 10 and lane 13, respectively. The results indicate two types of tertiary complexes: one is highly soluble (bound to Ca₄/CaM) and the other is much less soluble (bound to Ca₂/CaM₁₂ or Ca₂/CaM_C). Increasing the CaM concentration by 3-fold permitted Ca₂/CaM₁₂ (or Ca₂/CaM_C) to solubilize the majority of the tertiary complex as shown in Fig. 2B lane 10 and lane 13, respectively. However, the refolding of CT(1520–1669) with a 3-fold excess of CaM_C still had some precipitated tertiary complex CT(1520–1669):Ca₂/CaM_C (Fig. 2B lane 12). The increased solubility of CT(1520–1669) in the presence of 3-fold excess of Ca₂/CaM₁₂ might be caused by the artificial binding of two Ca₂/CaM₁₂ that bind to one CT(1520–1669). Indeed, our recent NMR structure of Ca₂/CaM₁₂ bound to the IQ peptide revealed that two Ca₂/CaM₁₂ can bind to one IQ peptide when the concentration of Ca₂/CaM₁₂ is more than 3-fold greater than the IQ peptide concentration [17]. We suggest that the binding of a second Ca₂/CaM₁₂ to CT(1520–1669) might mimic the binding of

Fig. 2. Ca²⁺-bound CaM promotes soluble refolding of CT(1520–1669). (A) SDS/PAGE monitoring the refolding of CT(1520–1669) in presence of Ca²⁺ free CaM (apoCaM), Ca₄/CaM, Ca₂/CaM₁₂, and Ca₂/CaM_C at 1 : 1 mixing ratio. Lane 1: Free unfolded CT(1520–1669) in 8 M urea, Lane 2: protein mass standards, Lane 3: total CT(1520–1669) mixture with apoCaM after dialysis, Lane 4: precipitated fraction of CT(1520–1669) refolded in the presence of apoCaM, Lane 5: solubilized fraction of CT(1520–1669) refolded in the presence of apoCaM, Lane 6: total CT(1520–1669) mixture with Ca₄/CaM after dialysis, Lane 7: precipitated fraction of CT(1520–1669) refolded in the presence of Ca₄/CaM, Lane 8: solubilized fraction of CT(1520–1669) refolded in the presence of Ca₄/CaM, Lane 9: total CT(1520–1669) mixture with Ca₂/CaM₁₂ after dialysis, Lane 10: precipitated fraction of CT(1520–1669) refolded in the presence of Ca₂/CaM₁₂, Lane 11: solubilized fraction of CT(1520–1669) refolded in the presence of Ca₂/CaM₁₂, Lane 12: total CT(1520–1669) mixture with Ca₂/CaM_C after dialysis, Lane 13: precipitated fraction of CT(1520–1669) refolded in the presence of Ca₂/CaM_C, Lane 14: solubilized fraction of CT(1520–1669) refolded in the presence of Ca₂/CaM_C, and Lane 15: free CaM. (B) SDS/PAGE monitoring the refolding of CT(1520–1669) in presence of Ca²⁺ free CaM (apoCaM), Ca₄/CaM, Ca₂/CaM₁₂, and Ca₂/CaM_C at 1 : 3 mixing ratio. Each experiment was repeated twice (*n* = 2). Lane 1: protein mass standards, Lane 2: total CT(1520–1669) mixture with apoCaM after dialysis, Lane 3: precipitated fraction of CT(1520–1669) refolded in the presence of apoCaM, Lane 4: solubilized fraction of CT(1520–1669) refolded in the presence of apoCaM, Lane 5: total CT(1520–1669) mixture with Ca₄/CaM after dialysis, Lane 6: precipitated fraction of CT(1520–1669) refolded in the presence of Ca₄/CaM, Lane 7: solubilized fraction of CT(1520–1669) refolded in the presence of Ca₄/CaM, Lane 8: total CT(1520–1669) mixture with Ca₂/CaM₁₂ after dialysis, Lane 9: precipitated fraction of CT(1520–1669) refolded in the presence of Ca₂/CaM₁₂, Lane 10: solubilized fraction of CT(1520–1669) refolded in the presence of Ca₂/CaM₁₂, Lane 11: total CT(1520–1669) mixture with Ca₂/CaM_C after dialysis, Lane 12: precipitated fraction of CT(1520–1669) refolded in the presence of Ca₂/CaM_C, Lane 13: solubilized fraction of CT(1520–1669) refolded in the presence of Ca₂/CaM_C, Lane 14: free Ca₂/CaM₁₂ and Lane 15: free Ca₂/CaM_C.



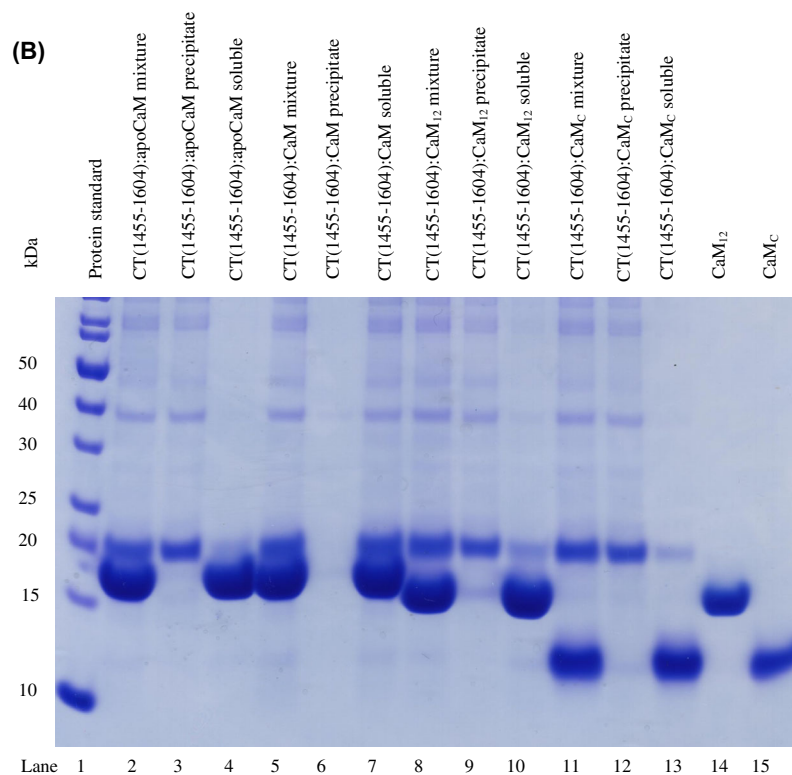
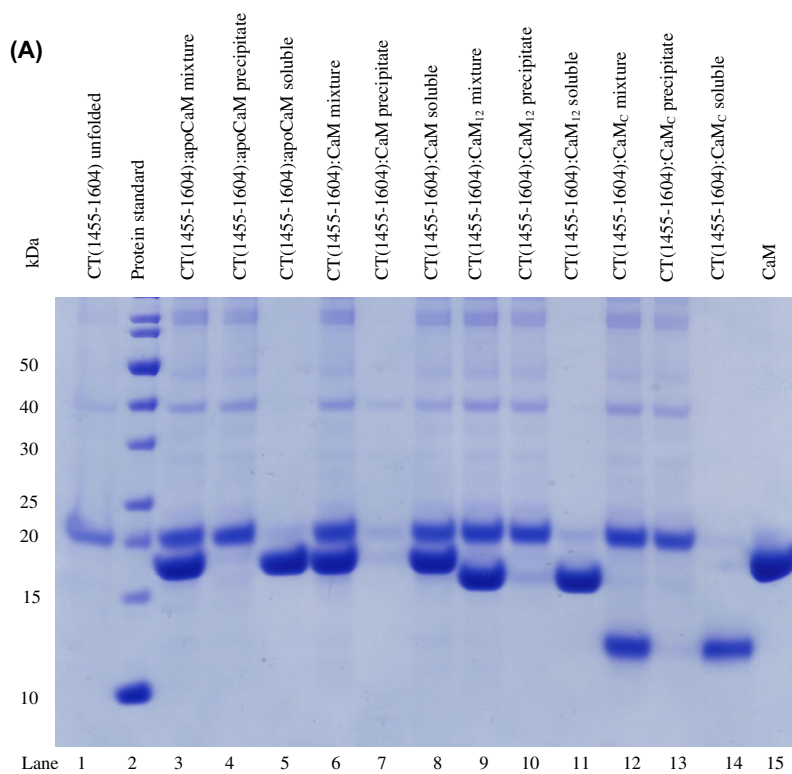


Fig. 3. Ca²⁺-bound CaM promotes soluble refolding of CT(1455–1604)^{CaV1.4}. (A) SDS/PAGE monitoring the refolding of CT(1455–1604) in presence of Ca²⁺ free CaM (apoCaM), calcified Ca₄/CaM, Ca₂/CaM₁₂, and Ca₂/CaM_C at 1 : 1 mixing ratio. Lane 1: Free unfolded CT(1455–1604) in 8 M urea, Lane 2: protein mass standards, Lane 3: total CT(1455–1604) mixture with apoCaM after dialysis, Lane 4: precipitated fraction of CT(1455–1604) refolded in the presence of apoCaM, Lane 5: solubilized fraction of CT(1455–1604) refolded in the presence of apoCaM, Lane 6: total CT(1455–1604) mixture with Ca₄/CaM after dialysis, Lane 7: precipitated fraction of CT(1455–1604) refolded in the presence of Ca₄/CaM, Lane 8: solubilized fraction of CT(1455–1604) refolded in the presence of Ca₄/CaM, Lane 9: total CT(1455–1604) mixture with Ca₂/CaM₁₂ after dialysis, Lane 10: precipitated fraction of CT(1455–1604) refolded in the presence of Ca₂/CaM₁₂, Lane 11: solubilized fraction of CT(1455–1604) refolded in the presence of Ca₂/CaM₁₂, Lane 12: total CT(1455–1604) mixture with Ca₂/CaM_C after dialysis, Lane 13: precipitated fraction of CT(1455–1604) refolded in the presence of Ca₂/CaM_C, Lane 14: solubilized fraction of CT(1455–1604) refolded in the presence of Ca₂/CaM_C, and Lane 15: free CaM. (B) SDS/PAGE monitoring the refolding of CT(1455–1604) in presence of Ca²⁺ free CaM (apoCaM), Ca₄/CaM, Ca₂/CaM₁₂, and Ca₂/CaM_C at 1 : 3 mixing ratio. Each experiment was repeated twice ($n = 2$) except for experiments with CaM_C ($n = 1$). Lane 1: protein mass standards, Lane 2: total CT(1455–1604) mixture with apoCaM after dialysis, Lane 3: precipitated fraction of CT(1455–1604) refolded in the presence of apoCaM, Lane 4: solubilized fraction of CT(1455–1604) refolded in the presence of apoCaM, Lane 5: total CT(1455–1604) mixture with calcified Ca₄/CaM after dialysis, Lane 6: precipitated fraction of CT(1455–1604) refolded in the presence of Ca₄/CaM, Lane 7: solubilized fraction of CT(1455–1604) refolded in the presence of Ca₄/CaM, 8: total CT(1455–1604) mixture with Ca₂/CaM₁₂ after dialysis, Lane 9: precipitated fraction of CT(1455–1604) refolded in the presence of Ca₂/CaM₁₂, Lane 10: solubilized fraction of CT(1455–1604) refolded in the presence of Ca₂/CaM₁₂, Lane 11: total CT(1455–1604) mixture with Ca₂/CaM_C after dialysis, Lane 12: precipitated fraction of CT(1455–1604) refolded in the presence of Ca₂/CaM_C, Lane 13: solubilized fraction of CT(1455–1604) refolded in the presence of Ca₂/CaM_C, Lane 14: free Ca₂/CaM₁₂ and Lane 15: free Ca₂/CaM_C.

the Ca²⁺-bound CaM N-lobe, which would cause the 1 : 2 complex (CT(1520–1669):(Ca₂/CaM₁₂)₂) to look structurally similar to the 1 : 1 complex (CT(1520–1669):Ca₄/CaM). Therefore, we suggest that a 1 : 1 complex of CT(1520–1669) bound to one Ca₂/CaM₁₂ (or Ca₂/CaM_C) is structurally distinct from the 1 : 1 complex of CT(1520–1669) bound to Ca₄/CaM. This is the first evidence that the structure of CT(1520–1669) bound to Ca₂/CaM₁₂ might be different from the structure of CT(1520–1669) bound to Ca₄/CaM.

The fact that apoCaM is not able to solubilize CT(1520–1669) is consistent with a low affinity binding of CT(1520–1669) to Ca²⁺-free CaM, as reported previously for apoCaM binding to the IQ peptide ($K_d \sim 10 \mu\text{M}$, [21]). Similar results were shown for CT(1513–1733). Again, apoCaM did not form a tertiary complex with CT(1513–1733) (Fig. S1A lane 5), whereas Ca₄/CaM formed a highly soluble tertiary complex (Fig. S1A lane 8). One equivalent of Ca₂/CaM₁₂ and Ca₂/CaM_C both form insoluble complexes with CT(1513–1733) (Fig. S1A lane 10 and lane 13) in contrast to the soluble complexes that formed in the presence of 3-fold excess Ca₂/CaM₁₂ or Ca₂/CaM_C (Fig. S1B lane 8 and lane 11).

Refolding of CT(1455–1604)^{CaV1.4} in the presence of Ca₄/CaM, Ca₂/CaM₁₂, and Ca₂/CaM_C

To check whether the C-terminal domain of the retinal L-type Ca²⁺ channel Ca_v1.4 (residues 1455–1604, called CT(1455–1604)^{CaV1.4}) can be solubilized by CaM, we performed similar refolding experiments with CT(1455–1604)^{CaV1.4} in the presence of apoCaM, Ca₂/CaM₁₂, Ca₂/CaM_C, and Ca₄/CaM as described above for CT(1520–1669). The refolding of urea-solubilized

CT(1455–1604)^{CaV1.4} in the presence of calcified CaMs caused formation of soluble tertiary complexes after removing urea by dialysis. By contrast, CT(1455–1604)^{CaV1.4} precipitated while dialysing away urea in the presence of apoCaM (Fig. 3A, lane 4). Adding 1 equivalent of Ca₄/CaM to urea-solubilized CT(1455–1604)^{CaV1.4} promoted the soluble refolding of a tertiary complex of CT(1455–1604)^{CaV1.4} bound to Ca₄/CaM (Fig. 3A, lane 8), whereas Ca₂/CaM₁₂ (or Ca₂/CaM_C) did not solubilize the tertiary complex (Fig. 3A lane 11 and lane 14, respectively). Adding 3 equivalents of Ca₂/CaM₁₂ (or Ca₂/CaM_C) to the urea-solubilized CT(1455–1604)^{CaV1.4} enabled soluble refolding of a much smaller fraction of tertiary complex (Fig. 3B lane 10 and lane 13, respectively) compared to that of Ca_v1.2 (Fig. 2B lane 10 and lane 13, respectively). The partial refolding of CT(1455–1604)^{CaV1.4} in the presence of half-calcified CaM suggests that Ca₂/CaM₁₂ forms a 2 : 1 complex with CT(1455–1604)^{CaV1.4} when the Ca₂/CaM₁₂ concentration is 3-fold higher than that of CT(1455–1604)^{CaV1.4}. This is the first evidence of two conformational states of CT(1455–1604)^{CaV1.4} that have different solubility.

NMR spectroscopy of CT(1520–1669) or CT(1455–1604)^{CaV1.4}/CT(1513–1733) bound to CaM

Ideally, we would like to solve the atomic-level structure of the tertiary complexes by NMR or X-ray crystallography. We screened thousands of conditions for crystallizing CT(1513–1733) bound to Ca₄/CaM, but so far none of these conditions produced any diffraction quality crystals. Instead, we performed SEC and ¹H-¹⁵N NMR HSQC on samples of ¹⁵N-labelled CT(1520–1669) bound to unlabelled Ca₂/CaM₁₂ or Ca₄/

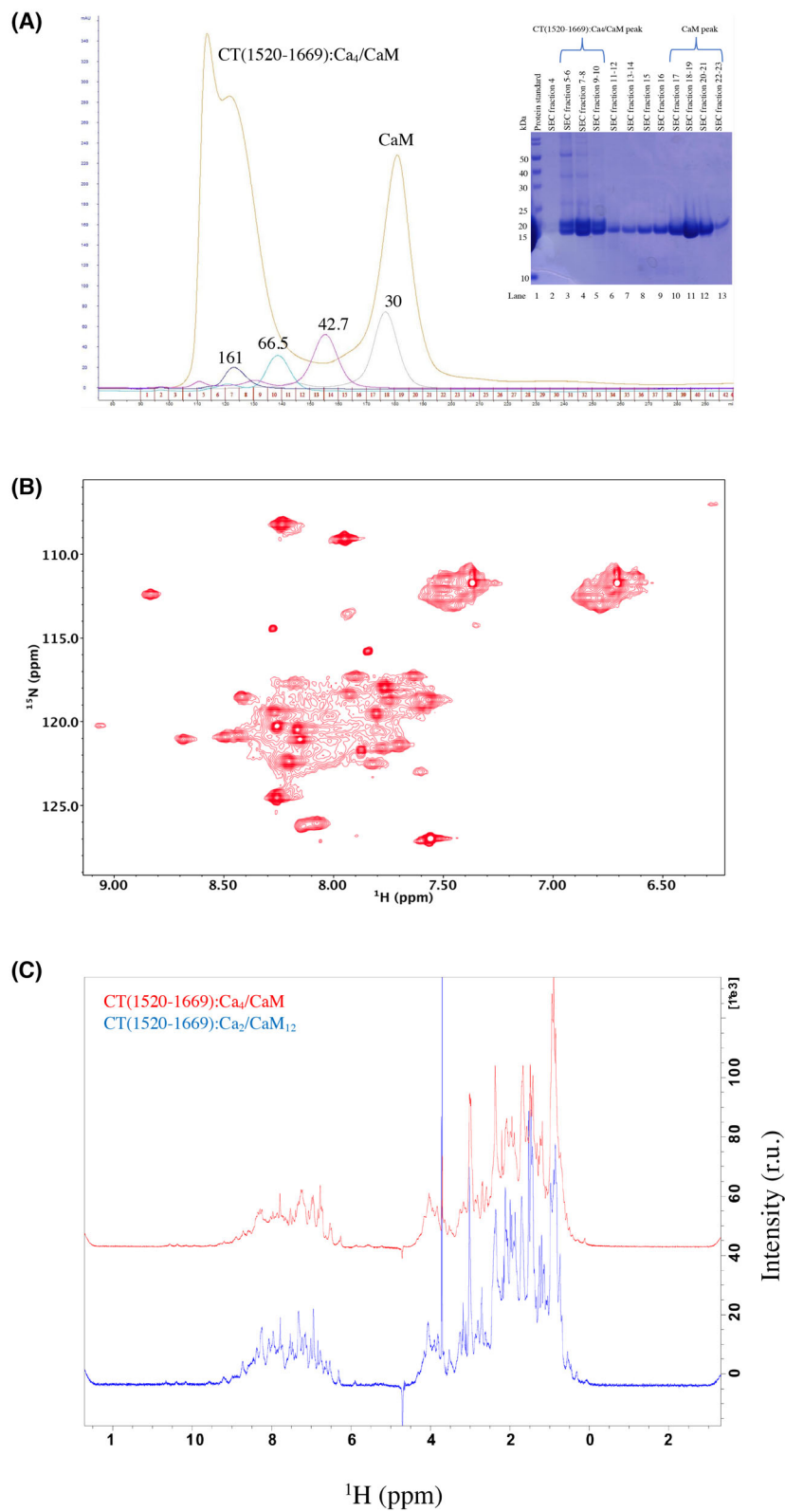


Fig. 4. NMR and SEC analysis of CT (1520–1669) binding to CaM. To determine the molar mass of the complex in solution, size exclusion chromatography (SEC) was run with Superdex 75 column in presence of 1 mM CaCl₂. SEC experiments were repeated twice ($n = 2$). (A) Curves from protein standards carbonic anhydrase (~ 30 kDa), chicken albumin (~ 43 kDa), bovine serum albumin (~ 66.5 kDa) and aldolase (~ 161 kDa) were overlaid with the CT(1520–1669):Ca₄/CaM complex of Ca_v1.2. SDS/PAGE was run after SEC to check the co-elution of both CT(1520–1669) and CaM in fractions were CT (1520–1669):Ca₄/CaM complex (fractions 5th to 10th) and access free CaM elution (fractions 17th to 23rd) peak observed, scanned SDS/PAGE gel picture is inserted in A right side. SEC fractions containing CT(1520–1669):Ca₄/CaM were pooled and concentrated to form the NMR sample. (B) 2D ¹H-¹⁵N HSQC NMR spectrum of ¹⁵N-labelled CT(1520–1669) bound to unlabelled Ca₄/CaM. (C) 1D proton NMR spectra of CT(1520–1669):Ca₄/CaM (red) and CT(1520–1669):Ca₂/CaM₁₂ (blue). Each NMR experiment was repeated twice ($n = 2$).

CaM (Fig. 4). The SEC chromatogram of CT(1520–1669) bound to Ca₄/CaM with protein standards indicates that the complex forms a mixture of tetramer or higher order oligomer (Fig. 4A). SDS/PAGE analysis of the SEC fractions confirmed the formation of a stable complex of CT(1520–1669) bound to Ca₄/CaM. CT(1520–1669) and Ca₄/CaM both co-elute as a complex (SEC fractions 5–10 in Fig. 4A) that is resolved from free CaM (SEC fractions 17–23 in Fig. 4A). The large size of the tetrameric complex explains why the HSQC NMR spectrum of ¹⁵N-labelled CT(1520–1669) (bound to unlabelled Ca₄/CaM) exhibits such broad NMR peaks (Fig. 4B). Interestingly, the amide peaks assigned to the IQ-motif were much sharper than the peaks from the channel EF-hand region, which suggests that the helical IQ-motif bound to Ca₄/CaM may exhibit segmental flexibility relative to the overall structure of the tetramer. A dynamically flexible and helical IQ-motif bound to Ca₄/CaM is consistent with the lack of electron density for the IQ-motif in the cryo-EM structure of Ca_v1.1 [14]. We could not obtain a 2D ¹H-¹⁵N HSQC NMR spectrum of the half-calcified tertiary complex (CT(1520–1669):Ca₂/CaM₁₂), due to its limited solubility. Instead, we recorded a 1D NMR spectrum of CT(1520–1669) bound to Ca₂/CaM₁₂, which looks somewhat different from the 1D NMR spectrum of CT(1520–1669) bound to Ca₄/CaM (Fig. 4C). The spectral differences are consistent with two distinct conformations of CT(1520–1669) bound to Ca₂/CaM₁₂ versus Ca₄/CaM, consistent with their different solubility. The 2D ¹H-¹⁵N HSQC NMR spectrum of CT(1513–1733):Ca₄/CaM complex (Fig. S2) shows additional amide peaks not seen in the spectrum of CT(1520–1669):Ca₄/CaM. The overlaid 2D ¹H-¹⁵N HSQC NMR spectra indicate amide peaks from CT(1520–1669):Ca₄/CaM (assigned to the IQ-motif) matched well with those of CT(1513–1733):Ca₄/CaM, whereas new amide peaks could be assigned to the PCRD domain (Fig. S2A). The 2D ¹H-¹⁵N HSQC NMR spectrum for CT(1455–1604)^{Ca_v1.4}:Ca₄/CaM complex (Fig. S2B) also exhibited very broad NMR signals like that seen for the Ca_v1.2 construct, and the broadness of the NMR peaks precluded doing a high-resolution atomic-level structural analysis of any of these complexes.

Discussion

In this study, we show that the C-terminal regulatory domain from Ca_v1.2 (CT(1520–1669)) and Ca_v1.4 (CT(1455–1604)) both form a soluble complex with half-calcified CaM (Ca₂/CaM₁₂) and fully calcified CaM (Ca₄/CaM) (Figs 2 and 3). By sharp contrast,

CT(1520–1669) cannot be solubilized in the presence of excess apoCaM, consistent with previous observations of low affinity apoCaM binding to the IQ-motif [21,24]. The CT(1520–1669):Ca₄/CaM complex is more soluble than CT(1520–1669):Ca₂/CaM₁₂, suggesting that CT(1520–1669) may adopt different structures when bound to Ca₂/CaM₁₂ versus Ca₄/CaM. Indeed, the NMR spectrum of CT(1520–1669):Ca₂/CaM₁₂ is somewhat different from that of CT(1520–1669):Ca₄/CaM (Fig. 4), consistent with a Ca²⁺-induced conformational change in CT(1520–1669) as predicted by Ames [6]. Both SEC and NMR suggest that a tetrameric CT(1520–1669) is bound to four CaM in a 4 : 4 complex (Fig. 4). The broad NMR resonances are consistent with a large 4 : 4 complex; however, a few sharp NMR peaks were assigned to residues in the IQ-motif bound to Ca₄/CaM. We suggest that the helical IQ-motif bound to Ca₄/CaM might be dynamically disordered in the complex to account for the sharp NMR linewidths, and these dynamics are consistent with the lack of electron density for the IQ-motif in the cryo-EM structure [14]. Lastly, the oligomerization of CT(1520–1669) (and CT(1513–1733)) suggests that the Ca_v1.2 C-terminal domain might make intermolecular contacts that could be important for channel clustering [25]. Future studies are needed to test the role of CT(1520–1669) in promoting channel clustering.

The different solubility between CT(1520–1669):Ca₂/CaM₁₂ and CT(1520–1669):Ca₄/CaM (Fig. 2) suggests that Ca²⁺ binding to the CaM N-lobe might trigger a conformational change in CT(1520–1669) (Fig. 5A,B). The previously proposed IQ-switch model for CDI [6] suggests that half-calcified CaM binding to the IQ-motif causes the sequestration of the IQ helix inside the channel EF-hands, in contrast to Ca₄/CaM binding that causes the IQ to flip outward and become solvent exposed. Hydrophobic residues in the IQ-motif (F1648, Y1649 and F1652) that are sequestered by their binding to the Ca₄/CaM N-lobe become solvent exposed upon binding to Ca₂/CaM₁₂, which might explain the higher solubility of CT(1520–1669):Ca₄/CaM compared to CT(1520–1669):Ca₂/CaM₁₂. The observation that a 3-fold excess of Ca₂/CaM₁₂ substantially increased the solubility of CT(1520–1669):Ca₂/CaM₁₂ (Fig. 2) suggests the formation of a 1 : 2 complex (Fig. 5C) that it is more soluble than the 1 : 1 complex (Fig. 5A). We suggest that the binding of a second Ca₂/CaM₁₂ to CT(1520–1669) (Fig. 5C) might resemble the binding of the Ca²⁺-bound CaM N-lobe to CT(1520–1669) in the 1 : 1 complex (Fig. 5B). This might explain why the 1 : 2 complex (CT(1520–1669):(Ca₂/CaM₁₂)₂, Fig. 5C) is more soluble than the 1 : 1 complex (CT(1520–1669):Ca₂/CaM₁₂, Fig. 5A). Future

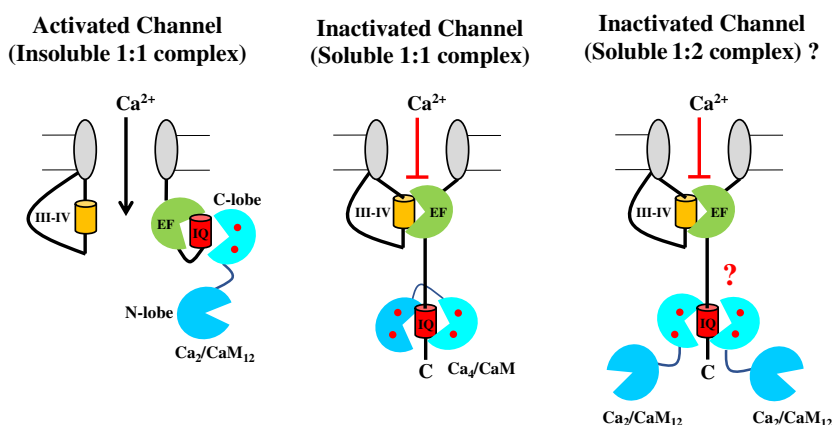


Fig. 5. Different solubility of CT(1520–1669):Ca₂/CaM₁₂ vs CT(1520–1669):Ca₄/CaM explained by a hypothetical IQ-switch model. (A) Channel activation at low Ca²⁺ concentration is caused by the binding of Ca₂/CaM₁₂ (cyan) to one side of the IQ-motif (red) while the other side of the IQ helix interacts with the channel EF-hand (green). (B) Channel inactivation at high Ca²⁺ concentration caused by the binding of Ca₄/CaM (cyan, dark blue) to both sides of the IQ helix, which causes extrusion of the IQ-motif from the channel EF-hand and allows the EF-hand to interact with the III–IV linker (orange) to form a plug at the entrance of the channel to block Ca²⁺ influx (red line). (C) Hypothetical channel inactivation state is suggested to cause artificial binding of two Ca₂/CaM₁₂ to one IQ-motif. The binding of a second Ca₂/CaM₁₂ to the IQ helix mimics the binding of Ca²⁺-bound CaM N-lobe (dark blue). The 1 : 2 complex (CT(1520–1669):(Ca₂/CaM₁₂)₂) is proposed to be soluble and only forms when an excess of CaM₁₂ is added to the channel. The 1 : 1 complex (CT(1520–1669):Ca₂/CaM₁₂) is proposed to be insoluble and forms when [Ca₂/CaM₁₂] is less than or equal to [CT(1520–1669)].

studies are needed to determine separate structures of CT(1520–1669) bound to Ca₂/CaM₁₂ and Ca₄/CaM.

The C-terminal regulatory domain of Ca_v1.2 (CT(1520–1669)) is about 90% identical in amino acid to that of Ca_v1.4 (Fig. 1B). The very high sequence identity suggests that CT(1520–1669) and CT(1455–1604)^{CaV1.4} should have a similar structure. Surprisingly, Ca_v1.4 does not exhibit channel CDI and does not bind to CaM in retinal photoreceptor cells. This lack of CaM binding to Ca_v1.4 is caused by a downstream domain in Ca_v1.4 (called ICDI) [26] which disables CaM binding. However, removal of the ICDI domain allows Ca_v1.4 to interact with CaM and restore CDI [27,28]. Consistent with these previous results, we find in our current study that CT(1455–1604)^{CaV1.4} (that lacks the ICDI domain) is structurally similar to CT(1520–1669)^{CaV1.2} (Fig. 4; Fig S2). However, an important structural difference is that the CT(1455–1604)^{CaV1.4}:Ca₂/CaM₁₂ is much less soluble than the CT(1520–1669)^{CaV1.2}:Ca₂/CaM₁₂ (Fig. 3). The lower solubility of CT(1455–1604)^{CaV1.4}:Ca₂/CaM₁₂ might indicate that the open conformation of Ca_v1.4 bound to Ca₂/CaM₁₂ (Fig. 5A) is more stable than the open conformation of Ca_v1.2 bound to Ca₂/CaM₁₂. We suggest that the open conformation of Ca_v1.4 bound to Ca₂/CaM₁₂ in the current study may be analogous to the open conformation of Ca_v1.4 bound to Ca₂/CaBP4 that exists in dark-adapted photoreceptors [29,30]. It makes sense that the open

conformation of Ca_v1.4 bound to Ca₂/CaBP4 would be more stable than the open state of Ca_v1.2 bound to Ca₂/CaM₁₂, because Ca_v1.4 needs to remain open for long periods in the dark-adapted photoreceptor, in contrast to the very short-lived open state of Ca_v1.2 in the brain. The increased stability of the open conformation of Ca_v1.4 bound to Ca₂/CaM₁₂ (or Ca₂/CaBP4) might explain why CT(1455–1604)^{CaV1.4} requires a higher concentration of Ca₂/CaM₁₂ to form the more soluble 1 & 2 complex (CT(1455–1604)^{CaV1.4}: (Ca₂/CaM₁₂)₂) that we suggest may represent the inactivated channel (Fig. 5C). Future structural studies on CT(1455–1604)^{CaV1.4} bound to CaM and/or CaBP4 are needed to test the prediction of our model.

Acknowledgements

This work was supported by NIH grants R01 EY012347 and R01 GM130925 (JBA) and RF1 AG055357 and R01 NS123050 (JWH). We thank Dr Ping Yu and Derrick Kaseman for help with NMR experiments performed at the UC Davis NMR Facility.

Author contributions

DKY, JBA, and JWH designed and wrote the paper; DKY and JBA performed experiments; DKY and DEA performed subcloning, DKY, DEA, JWH, and JBA analysed data.

Data accessibility

The data that support the findings of this study are available in the main figures and the supplementary material of this article.

References

- 1 Striessnig J, Pinggera A, Kaur G, Bock G, Tuluc P. L-type Ca²⁺ channels in heart and brain. *Wiley Interdiscip Rev Membr Transp Signal*. 2014;**3**:15–38.
- 2 Wheeler DG, Groth RD, Ma H, Barrett CF, Owen SF, Safa P, et al. CaV1 and CaV2 channels engage distinct modes of Ca²⁺ signaling to control CREB-dependent gene expression. *Cell*. 2012;**149**:1112–24.
- 3 Lewis BB, Wester MR, Miller LE, Nagarkar MD, Johnson MB, Saha MS. Cloning and characterization of voltage-gated calcium channel alpha1 subunits in *Xenopus laevis* during development. *Dev Dyn*. 2009;**238**:2891–902.
- 4 Wheeler DB, Randall A, Tsien RW. Roles of N-type and Q-type Ca²⁺ channels in supporting hippocampal synaptic transmission. *Science*. 1994;**264**:107–11.
- 5 Simms BA, Souza IA, Rehak R, Zamponi GW. The Cav1.2 N terminus contains a CaM kinase site that modulates channel trafficking and function. *Pflug Arch*. 2014;**467**:677–86.
- 6 Ames JB. L-type Ca²⁺ channel regulation by calmodulin and CaBP1. *Biomolecules*. 2021;**11**:1811.
- 7 Christel C, Lee A. Ca²⁺-dependent modulation of voltage-gated Ca²⁺ channels. *Biochim Biophys Acta*. 2012;**1820**:1243–52.
- 8 Nanou E, Catterall WA. Calcium channels, synaptic plasticity, and neuropsychiatric disease. *Neuron*. 2018;**98**:466–81.
- 9 Adams PJ, Johny M, Dick I, Inoue T, Yue DT. Apocalmodulin itself promotes ion channel opening and Ca²⁺ regulation. *Cell*. 2014;**159**:608–22.
- 10 Splawski I, Timothy KW, Sharpe LM, Decher N, Kumar P, Bloise R, et al. CaV1.2 calcium channel dysfunction causes a multisystem disorder including arrhythmia and autism. *Cell*. 2004;**119**:19–31.
- 11 Bader PL, Faizi M, Kim LH, Owen SF, Tadross MR, Alfa RW, et al. Mouse model of Timothy syndrome recapitulates triad of autistic traits. *Proc Natl Acad Sci USA*. 2011;**108**:15432–7.
- 12 Cain SM, Snutch TP. Voltage-gated calcium channels and disease. *Biofactors*. 2011;**37**:197–205.
- 13 Wu J, Yan Z, Li ZQ, Yan C, Lu S, Dong MQ, et al. Structure of the voltage-gated calcium channel Cav1.1 complex. *Science*. 2015;**350**:aad2395.
- 14 Wu J, Yan Z, Li ZQ, Qian XY, Lu S, Dong MQ, et al. Structure of the voltage-gated calcium channel Ca_v1.1 at 3.6 Å resolution. *Nature*. 2016;**537**:191–6.
- 15 Van Petegem F, Chatelain FC, Minor JDL. Insights into voltage-gated calcium channel regulation from the structure of the CaV1.2 IQ domain–Ca²⁺/calmodulin complex. *Nat Struct Mol Biol*. 2005;**12**:1108–15.
- 16 Xiong L, Kleerekoper QK, He R, Putkey JA, Hamilton SL. Sites on calmodulin that interact with the C-terminal tail of Cav1.2 channel. *J Biol Chem*. 2005;**280**:7070–9.
- 17 Bartels P, Salveson I, Coleman AM, Anderson DE, Jeng G, Estrada-Tobar ZM, et al. Half-calcified calmodulin promotes basal activity and inactivation of the L-type calcium channel Ca_v1.2. *bioRxiv*. 2022. <https://doi.org/10.1101/2022.06.24.497440>
- 18 Arbing MA, Chan S, Harris L, Kuo E, Zhou TT, Ahn CJ, et al. Heterologous expression of mycobacterial Esx complexes in *Escherichia coli* for structural studies is facilitated by the use of maltose binding protein fusions. *PLoS One*. 2013;**8**:e81753.
- 19 Klock HE, Lesley SA. The polymerase incomplete primer extension (PIPE) method applied to high-throughput cloning and site-directed mutagenesis. *Methods Mol Biol*. 2009;**498**:91–103.
- 20 Li MZ, Elledge SJ. SLIC: a method for sequence- and ligation-independent cloning. *Methods Mol Biol*. 2012;**852**:51–9.
- 21 Turner M, Anderson DE, Bartels P, Nieves C, Andrea MC, Henderson PB, et al. α -Actinin-1 promotes gating of the L-type Ca²⁺ channel CaV1.2. *EMBO J*. 2020;**39**:e102622.
- 22 Norris M, Fetler B, Marchant J, Johnson BA. NMRFX processor: a cross-platform NMR data processing program. *J Biomol NMR*. 2016;**65**:205–16.
- 23 Johnson BA. Using NMRView to visualize and analyze the NMR spectra of macromolecules. *Methods Mol Biol*. 2004;**278**:313–52.
- 24 Evans TIA, Hell JW, Shea MA. Thermodynamic linkage between calmodulin domains binding calcium and contiguous sites in the C-terminal tail of CaV1.2. *Biophys Chem*. 2011;**159**:172–87.
- 25 Dixon RE, Moreno CM, Yuan C, Opitz-Araya X, Binder MD, Navedo MF, et al. Graded Ca²⁺/calmodulin-dependent coupling of voltage-gated CaV1.2 channels. *Elife*. 2015;**4**:e05608.
- 26 Wahl-Schott C, Baumann L, Cuny H, Eckert C, Griessmeier K, Biel M. Switching off calcium-dependent inactivation in L-type calcium channels by an autoinhibitory domain. *Proc Natl Acad Sci USA*. 2006;**103**:15657–62.
- 27 Liu X, Yang PS, Yang W, Yue DT. Enzyme-inhibitor-like tuning of Ca(2+) channel connectivity with calmodulin. *Nature*. 2010;**463**:968–72.
- 28 Sang L, Vieira DCO, Yue DT, Ben-Johny M, Dick IE. The molecular basis of the inhibition of Ca_v1 calcium-

- dependent inactivation by the distal carboxy tail. *J Biol Chem.* 2021;**296**:100502.
- 29 Haeseleer F, Imanishi Y, Maeda T, Possin DE, Maeda A, Lee A, et al. Essential role of Ca²⁺-binding protein 4, a Cav1.4 channel regulator, in photoreceptor synaptic function. *Nat Neurosci.* 2004;**7**:1079–87.
- 30 Park S, Li C, Haeseleer F, Palczewski K, Ames JB. Structural insights into activation of the retinal L-type Ca²⁺ channel (Cav1.4) by Ca²⁺-binding protein 4 (CaBP4). *J Biol Chem.* 2014;**289**:31262–73.

Supporting information

Additional supporting information may be found online in the Supporting Information section at the end of the article.

Fig. S1. Ca²⁺-bound CaM promotes soluble refolding of CT(1513-1733) Ca_v1.2.

Fig. S2. 2D ¹H-¹⁵N HSQC NMR of CT(1520-1669) (or CT(1455-1604)/CT(1513-1733)) bound to CaM.